Progress In Electromagnetics Research Letters, Vol. 21, 19–29, 2011

A HIGH-RATIO BANDWIDTH SQUARE-WAVE-LIKE BANDPASS FILTER BY TWO-HANDED METAMATERIALS AND ITS APPLICATION IN 60 GHZ WIRELESS COMMUNICATION

T.-Y. Huang and T.-J. Yen

Department of Materials Science and Engineering
National Tsing Hua University
101, Section 2, Kuang Fu Road, Hsinchu 30013, Taiwan, R.O.C.

Abstract—By enabling both cavity modes and plasmonic resonance together in the designed two-handed metamaterial, we demonstrate a square-wave-like (SWL) bandpass filter with high-ratio bandwidth (HRB). Our results show that this metamaterial-based bandpass filter possesses high-ratio bandwidth of 30 GHz centered at 92 GHz, excellent transmittance beyond 87.5%, sharp transition within 1.0 GHz from -3 dB to -20 dB as upper and lower band edge transitions, and dual-band behavior. Such an HRBSWL bandpass filter can be scalable and readily applicable for the commercialized unlicensed 60 GHz spectra with a bandwidth exceeding 7 GHz, solving the challenge of conventional passive bandpass filters to allow wide bandwidths and great quality factors simultaneously.

1. INTRODUCTION

To ease the congestion of local area network (LAN) and to pursue high definition (HD) quality of cinema, currently researchers are eager to realize the next generation high speed wireless communication technology. There appear several competing solutions beyond the current Wi-Fi system, in particular ultrawide band (UWB) [1] and 60 GHz techniques [2]. The former, namely exhibiting an effective bandwidth at least 20% greater than its operating frequency, is achieved by broadcasting pulses with a full duration at half maximum (FDHM) about several-hundred picoseconds and then Fourier transformed into wide frequency range signals. Certainly

Received 17 November 2010, Accepted 24 January 2011, Scheduled 16 February 2011
Corresponding author: Ta-Jen (David) Yen (tjyen@mx.nthu.edu.tw).

the UWB technique possesses better security and higher data rate than the conventional Wi-Fi system, but its allowed spectra differ in various countries, resulting in the difficulties to establish a standard prototype [3]. The latter, on the other hand, operated within the unlicensed spectrum centered at 60 GHz with a bandwidth exceeding 7 GHz ruled by federal communication constitute (FCC) [3], becomes the most promising candidate currently because it provides highest transmission rate than other wireless techniques that even ensures to transmit uncompressed HD data and more importantly, it has been supported by many mainstream companies recently [4].

For wireless communication applications, a bandpass filter is a crucial and mass-used component to allow signals and to suppress noises in the specific frequencies [5], and so far, it remains a challenge to realize a suitable bandpass filter for the 60 GHz technique to satisfy the demanding requirements of sharp bandedge transition [6–9], high-ratio bandwidth, and excellent transmittance efficiency [6, 7]. Here, we introduce a new class of metamaterials to demonstrate right-handed response from its cavity modes and left-handed response from its plasmonic resonance simultaneously, leading the collective two-handed response to constructing a high-ratio bandwidth (HRB) bandpass filter [10]. In addition, due to the transition between the right-handed and left-handed response, such a device spontaneously matches the wave impedance to enhance its transmittance efficiency [10]. Finally, it owns a further advantage of sharp bandedge transition due to the resonant characteristics of metamaterials, providing an HRBSWL solution to solving the challenge aforementioned.

2. DESIGN AND NATURE OF TWO-HANDED METAMATERIALS

For a conventional bandpass filter, there exists a tradeoff between its bandwidth and quality factor expressed by the following formula,

$$B.W. = \frac{f_0}{Q} \tag{1}$$

where $B.W.$ is the bandwidth, f_0 the central frequency and Q the quality factor of the filter. To overcome these fundamentally incompatible properties — that is, demonstrating a high-ratio bandwidth bandpass filter with high quality factor simultaneously — we combine the left-handed plasmonic resonance induced by effective inductance-capacitance circuits in two metal layers, and right-handed performance created by cavity modes in the dielectric part together [9–13] as shown in Fig. 1. The designed HRBSWL bandpass filter is

Table 1. The detailed geometric parameters of the unit cell. (Set A is used for experimental evidence while Set B is used for application in 60 GHz.)

Parameters	Set A (75–110 GHz; mm)	Set B (50–75 GHz; mm)
a_x	2	3
a_y	2	3
l	1.67	2.5
w	0.67	1
m	0.067	0.1

tailored by two metal plates of 8 µm thick with hollowed crossed bars in the center, sandwiching a commercially available Roger board 5880 whose thickness and dielectric constant (ε_r) are 0.254 mm and 2.2, respectively. The detailed geometric parameters are presented in Table 1. Limited by our measurement equipment, we fabricate the HRBSWL filter with the parameters of Set A to comply with the measurable range from 75 GHz to 110 GHz, but one can easily shift the operating frequency, for example to 60 GHz by scaling the geometric parameters as shown in Set B, stemming from the scalable characteristics of two-handed metamaterial (THM) [14]. In the design process, we employ a commercialized electromagnetic solver CST Microwave Studio to compute the complex reflectance and transmittance coefficients, and also scrutinize field distributions and induced surface current in this HRB bandpass fitler to identify the respective right-handed and left-handed properties at different frequencies.

In fact, the enabling factor of this HRBSWL filter is based on the collective response of the individual right-handed and left-handed properties to construct a two-handed metamaterial. The right-handed property stems from the cavity modes existing in the dielectric region of the unit cell, which contributes complex electric permittivity and non magnetic behavior to a passband, and the allowed frequencies of this passband is further determined by the dimension of the hollowed crossed bars presented in Fig. 1 and Table 1. Meanwhile, for left-handed property, the metal plates provide an effective permittivity depicted by Drude's model [15–17],

$$\varepsilon_{eff}(\varpi) = 1 - \frac{\varpi_p^2}{\varpi^2 + i\Gamma_E \varpi} \tag{2}$$

where ω_p is the new plasma frequency governed by the designed pattern of the metal plates and Γ_E is electrical resistive loss in the resonating

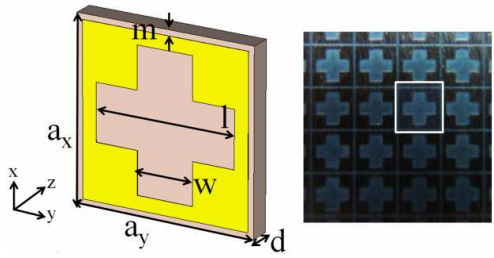

Figure 1. The unit cell of the designed high-ratio bandwidth square-wave-like (HRBSWL) bandpass filter and its perspective view. (a) The yellow parts are two patterned copper plates of 0.008 mm thickness, sandwiching a Roger board 5880 substrate of 0.254 mm thickness with the relative dielectric constant of 2.2 in simulation. (b) The optical image of the sample fabricated by a print-circuit-board technique. Here the black region is the opaque copper plate. All the geometric parameters are tabulated in Table 1.

system. Moreover, the paired metal plates introduce anti-parallel surface currents, functioning as Lorentz oscillators to create an effective permeability expressed by Lorentz model [15–18],

$$\mu_{eff}(\varpi) = 1 - \frac{\varpi_{MP}^2 - \varpi_{M0}^2}{\varpi^2 - \varpi_{M0}^2 + i\Gamma_M \varpi} \tag{3}$$

where ω_{MP} denotes magnetic plasma frequency, ω_{M0} resonant frequency of magnetic dipole, and Γ_M magnetic resistive loss. By harvesting the effective negative values of permittivity and permeability region together in their overlapped frequencies, one will accomplish a left-handed passband with a negative refractive index.

3. SAMPLE FABRICATION AND MEASURED RESULTS

The designed HRBSWL filter was fabricated by means of commercial printed-circuit-board technology, whose sample size is 107 mm × 107 mm (50 × 50 unit cells in total) as shown in Fig. 1. Besides, the fabricated samples were characterized by an N5260A PNA series network analyzer attached with mixers and standard gain horn antennas to generate electromagnetic waves and to emit plane waves within frequencies from 75 to 110 GHz. We measured both the magnitude of transmittance (i.e., S_{21} parameter) and the phase of transmittance (i.e., arg S_{21}) at normal incidence. As shown in Fig. 2,

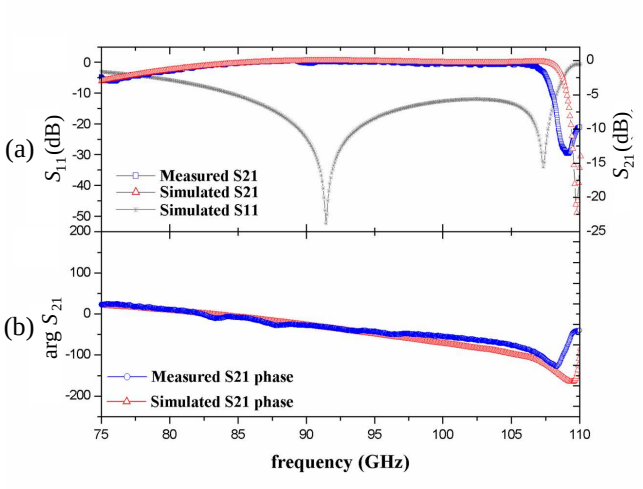

Figure 2. (a) The simulated transmittance (red line), reflectance (gray dashed line) and measured transmittance (blue line) curves in dB scale at normal incidence for single layer. We observe sharp bandedge transition at upper bound, and a near zero transmittance band within 75–105 GHz indicating a high-ratio bandwidth allowed band in this frequency region. (b) The phase of transmittance change of simulation (red line) and measurement (blue line). The experimental and simulation results agree each other well with a sharp phase change from a resonant behavior of THM.

it is clear to observe that a single board of HRB filter yields a high-ratio bandwidth greater than 30 GHz (from 75.91 to 107.73 GHz) as a consequence of two-handed response as expected. In addition, the transmittance efficiency exceeds 96% through the entire high-ratio band because a quasi wave impedance match occurs to spontaneously depress reflectance (0.0026%), we achieve high transmittance efficiency (99.67%) [10]. Finally, a sharp upper bandedge transition of 17 dB/GHz, resulting from a resonance indicated by the sudden phase change of transmittance shown in Fig. 2(b). The experimental results agree well with simulation data. Here exists a little shift regarding the frequency of stop band and the slope of phase transition owing to the different values of dielectric constants of Roger board 5880 and spacing between two horn antennas in simulation and practical cases.

Next, we scrutinize the field distributions based on reflectance dips located at 91.4 and 107.38 GHz, and surface currents about transmission dips for lower and upper stop bandedges located at 74.86 and 109.94 GHz, respectively. First of all, we observe parallel

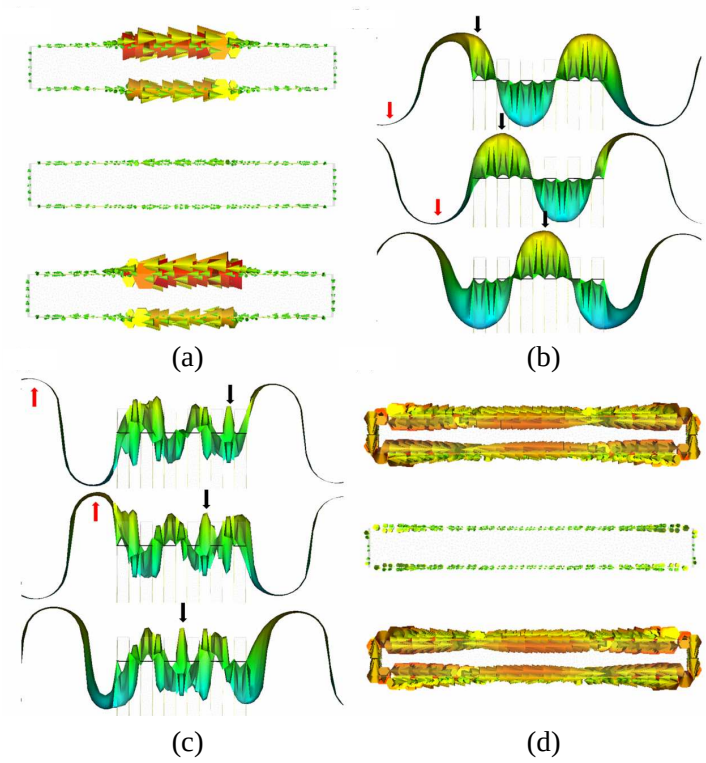

Figure 3. (a) Snapshot of top view of induced surface current at 74.86 GHz. A parallel surface currents demonstrate that a negative permittivity results in a stop band. (b) Snapshot of side view of E field distribution at 91.4 GHz. The red arrows represent peak of the wave within free space and black arrows indicate peak of the wave within metamaterial. The same direction of phase velocity between region of free space and metamaterial demonstrate that the right-handed allowed band is composed of positive permittivity and permeability. (c) Snapshot of side view of E field distribution at 107.38 GHz. In contrary to Fig. 3(b), the opposite directions of phase velocity demonstrate that the left-handed allowed band is composed of negative permittivity and permeability. (d) Snapshot of top view of surface current at 109.94 GHz. The anti-parallel surface current result in a negative permeability to form a stop band.

induced surface current at 74.86 GHz as shown in Fig. 3(a) which result in negative permittivity to form a stop band. Next, there appears right-handed allowed band at 91.4 GHz evidenced by the

same direction of phase velcocity between regions of free space and metamaterial as shown in Fig. 3(b) representing both positive permittivity and permeability within the band. In addition to the right-handed response, the SWL filter exhibits negative permittivity and permeability as a left-handed allowed band evidented by the opposite directions of phase velocity as shown in Fig. 3(c). Finally, the anti-parallel induced surface currents result in a negative permeability to form a stop band at 109.94 GHz as shown in Fig. 3(d).

From the E and H field distributions at these four different frequencies, we conclude that this HRB filter is composed of lower stop band edged at 91.4 GHz due to negative permittivity, right-handed, left-handed allowed bands and finally upper stop band edged at 107.38 GHz due to negative permeability to form a well behaved two-handed HRB bandpass filter.

Notice that the upper bound (i.e., left-handed response) presents sharper bandedge transition than the lower one because of plasmonic resonance described by Eq. (3), Fig. 2(b), and Fig. 3(d). Therefore, to enhance the bandedge transition of the lower bound, we increase the number of boards to hire Fabry-Pérot interference to sharpen that transition, and gain an additional merit of greater bandedge transition for the lower stop band as shown in Fig. 4(a). Yet, such enhancement is sensitive to the distances among boards, so that the measurement does not match simulation well caused by the difficulty to manually control the distance among boards precisely. We also calculate corresponding group delay time within two-handed HRB bandpass filter via phase of S_{21} in simulation. As shown in Fig. 4(c), this HRB filter maintains homogenous group delay time less than 0.1 ns through the entire allowed band, leading nearly no frequency dispersion to the freedom from integrating an extra optical delay line to render signals arriving the other end at the same time.

Finally, we unveil the general response about two scalable HRB filters (listed in Table 1) from 1 GHz to 120 GHz as shown in Fig. 5, especially the case of Set B, which can be readily applied in the upcoming 60 GHz techniques. As shown in Fig. 5(b), a major allowed band locates between 50 to 72.5 GHz, a hot zone for unlicensed spectrum centered at 60 GHz with exceeding 7 GHz bandwidth to enable that the transmission rate are up to 5 Gbps. Here the effective ratio of bandwidth to centered frequency is up to 33%, much better than UWB technique, with which one could achieve 20% bandwidth at its the centered frequency (in the range of 3.1 to 10.6 GHz). In addition to the unprecedented allowed band with square-function shapes to demonstrate high-ratio bandwidth, excellent transmittance efficiency and sharp bandedge transition, it is also interesting that these

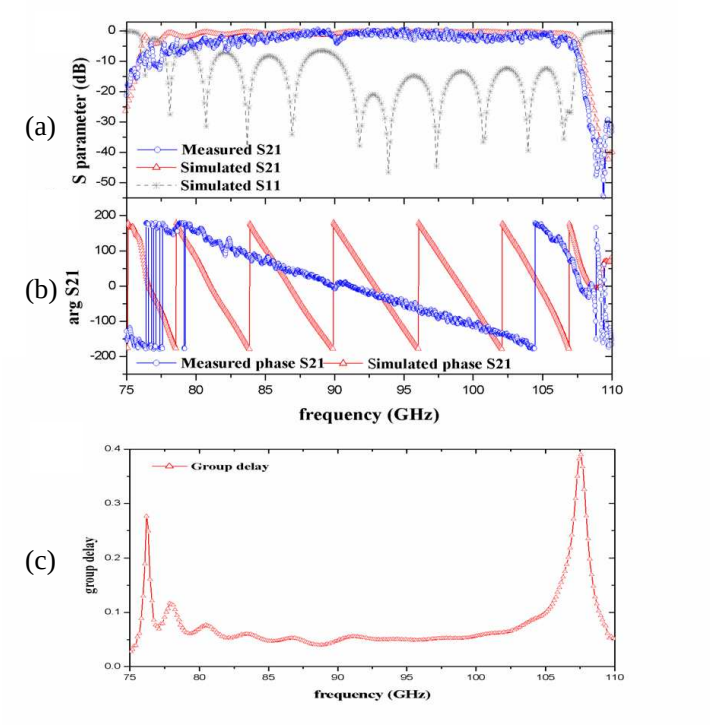

Figure 4. (a) The S-parameter magnitudes of the two-handed high-ratio bandwidth bandpass filter in the numerical simulations (red line for S_{21} and gray-dash line for S_{11}) and the real measurements (blue solid lines) for 5-layer unit cells with distance 'd' equals to 5 mm under normal incidence condition. The effective bandwidth exceeds 30 GHz with sharper band edge transition. (b) The simulated (red line) and measured (blue line) phase of transmittance. (c) The corresponding group delay calculated by phase of transmittance in simulation. Within allowed band, we obtain almost homogenous value of group delay, which will render delay lines excrescent in the module of wireless communication industry.

HRB bandpass filters give rise to an additional allowed band between 1 GHz and 9 GHz that act as a low-pass filter to cover the frequency ranges operated by the current commercialized wireless communication products such as Wi-Fi and Bluetooth. In this manner, our device can be switched to Wi-Fi bands to continue filtering out undesired signals as the transmission of 60 GHz is blocked by obstacles due to its high directivity, realizing a dual-band solution suggested by mainstream alliance to ease a major concern of 60 GHz techniques [19].

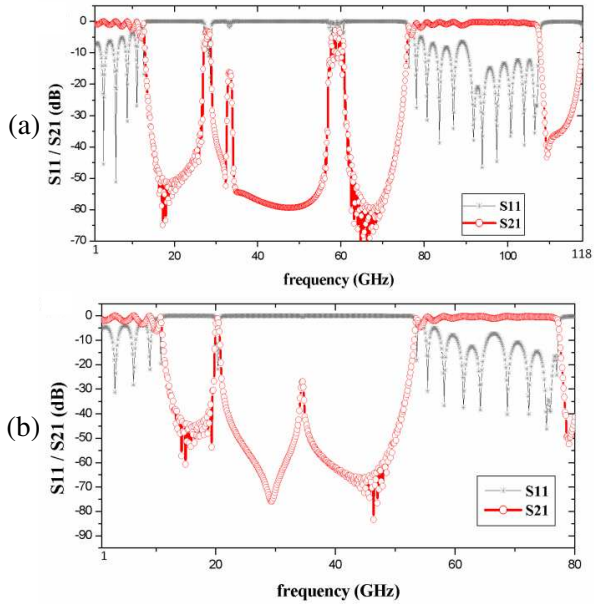

Figure 5. Diagram of complex transmittance for two sets of frequencies, 50 to 75 GHz and 75 to 110 GHz, respectively. (a) A multi-allowed band bandpass filter is presented. The first allowed band is located at 1-12.5 GHz and second allowed band range from 77.5 to 107.5. (b) the transmittance with the other parameters of unit cell as shown in Table 1, and we can observe that the first allowed band is also existing within 1 to 9 GHz and is useful for commercialized Wi-Fi, Bluetooth technology, and the second allowed band is located at from 50 to 72.5 GHz and is suitable for 60 GHz unlicensed spectrum. The two figures also show scalable properties of the two-handed HRB filter.

4. CONCLUSIONS

In this work, we design a scalable two-handed metamaterial to successfully demonstrate an unprecedent bandpass filter with high-ratio bandwidth, excellent transmission efficiency, and sharp bandedge transition in both numerical simulation and experimental measurements. Such an HRB filter possesses a square-function-like passband and contains a high-ratio bandwidth (exceeding 30 GHz), excellent efficiency (above 87.5%) and high selectivity factor simultaneously. Besides, multi-allowed transmission bands of the filter are suitable for the existing commercialized wireless technology and also cover frequency of 60 GHz ranges, which is the most potential

technology for next generation wireless communication. Therefore, we expect once we apply this HRBSWL filter in the module of wireless communication products, we can reduce the volume of devices and lower the power emitted from antennas due to much higher transmittance and result in much competitive products used in next generation Wi-Fi, Bluetooth and others.

ACKNOWLEDGMENT

The authors would like to gratefully acknowledge the financial support from National Science Council (NSC98-2112-M-007-002MY3, NSC99-2120-M-002-012 and NSC99-2120-M-010-001), and Ministry of Economic Affairs (98-EC-17-A-08-S1-003).

REFERENCES

1. http://www.palowireless.com/uwb/tutorials.asp.
2. http://spectrum.ieee.org/consumer-electronics/standards/gadgets-gab-at-60-ghz.
3. http://en.wikipedia.org/wiki/Ultra-wideband.
4. http://www.wirelesshd.org/membership/.
5. Wang, X.-H., B.-Z. Wang, and K. J. Chen, "Compact broadband dual-band bandpass filters using slotted ground structures," *Progress In Electromagnetics Research*, Vol. 82, 151–166, 2008.
6. Yang, B., E. Skafidas, and R. J. Evans, "Design of 60 GHz millimetre-wave bandpass filter on bulk CMOS," *IET Microwaves Antennas & Propagation*, Vol. 3, 943–949, 2009.
7. Yao, B. Y., Y. G. Zhou, Q. S. Cao, and Y. C. Chen, "Compact UWB bandpass filter with improved upper-stopband performance," *IEEE Microw. Wirel. Compon. Lett.*, Vol. 19, 27–29, 2009.
8. Razalli, M. S., A. Ismail, M. A. Mahdi, and M. N. Bin Hamidon, "Novel compact microstrip ultra-wideband filter utilizing short-circuited stubs with less vias," *Progress In Electromagnetics Research*, Vol. 88, 91–104, 2008.
9. Ma, K. X., K. C. B. Liang, R. M. Jayasuriya, and K. S. Yeo, "A wideband and high rejection multimode bandpass filter using stub perturbation," *IEEE Microw. Wirel. Compon. Lett.*, Vol. 19, 24–26, 2009.
10. Chiang, Y.-J. and T.-J. Yen, "A highly symmetric two-handed

metamaterial spontaneously matching the wave impedance," *Opt. Express*, Vol. 16, 12764–12770, 2008.

11. Fu, L., H. Schweizer, H. Guo, N. Liu, and H. Giessen, "Synthesis of transmission line models for metamaterial slabs at optical frequencies," *Phys. Rev. B*, Vol. 78, 9, 2008.
12. Cimen. S., G. Cakir, and L. Sevgi, "Metamaterial slabs and realization of all-type filter characteristics: Numerical and analytical investigations," *Microwave and Optical Technology Letters*, Vol. 51, 894–899, 2009.
13. Fu,, L., H. Schweizer, H. Guo, N. Liu, and H. Giessen, *Analysis of Metamaterials Using Transmission Line Models*, 425–429, Springer, 2007.
14. Yen, T. J., W. J. Padilla, N. Fang, D. C. Vier, D. R. Smith, J. B. Pendry, D. N. Basov, and X. Zhang, "Terahertz magnetic response from artificial materials," *Science*, Vol. 303, 1494–1496, 2004.
15. Smith, D. R., D. C. Vier, T. Koschny, and C. M. Soukoulis, "Electromagnetic parameter retrieval from inhomogeneous metamaterials," *Physical Review E*, Vol. 71, 11, 2005.
16. Chen, X. D., T. M. Grzegorczyk, B. I. Wu, J. Pacheco, and J. A. Kong, "Robust method to retrieve the constitutive effective parameters of metamaterials," *Physical Review E*, Vol. 70, 7, 2004.
17. Ziolkowski, R. W., "Design, fabrication, and testing of double negative metamaterials," *IEEE Trans. Antennas Propag.*, Vol. 51, 1516–1529, 2003.
18. Koschny, T., M. Kafesaki, E. N. Economou, and C. M. Soukoulis, "Effective medium theory of left-handed materials," *Phys. Rev. Lett.*, Vol. 93, 107402, 2004.
19. http://www.itexaminer.com/intel-rd-says-60ghz-wireless-is-way-to-go-.aspx.